Alternative Direct Sampling Method in 3D Inverse Electromagnetic Scattering Problem

Sangwoo Kang, Marc Lambert

Alternative Direct Sampling Method in 3D Inverse Electromagnetic Scattering Problem

Sangwoo Kang, and Marc Lambert
Group of Electrical Engineering, Paris (GeePs), UMR CNRS 8507, CentraleSupélec, Univ. Paris Sud, Université Paris Saclay, Sorbonne Universités, UPMC Univ Paris 06, 3 & 11 rue Joliot-Curie 91192, Gif-sur-Yvette, France

***Abstract*—In the following the recently developed direct sampling method for solving 3D inverse electromagnetic scattering problem is dealt with and an alternative indicator function decreasing the artifacts is proposed. The latter is an extension of an alternative direct sampling method recently proposed for 2D inverse acoustic case. Due to the vectorial aspect of the 3D problem the imaging test functions have to be carefully handled. Numerical simulations with synthetic data are provided to verify our suggestion and compare the result with original DSM.**

***Index Terms*—Inverse electromagnetic scattering problem, Non-iterative method, Dyadic green function, Numerical simulation.**

I. Introduction

The main purpose of inverse electromagnetic scattering problem is to retrieve the informations (location, shape, permittivity, etc.) of one of more targets from the measured electromagnetic scattered data. Due to its various applications, for example, non-destructive testing [1], and biomedical imaging for detecting breast cancer [2], etc., analysis and development of efficient techniques have been attracting research topic.

Many of such algorithms, for instance, MUltiple SIgnal Classification (MUSIC), linear sampling method (LSM), and migration-type method (Kirchhoff migration, subspace migration), etc, have good results to reconstruct the shapes and locations of unknown targets with sufficient many incident fields [3]–[5], bu can faill otherwise [5].

To overcome this difficulty, a new sampling type method, so called direct sampling method (DSM), has recently been developed for 2D and 3D inverse scattering problem [6], [7]. According to [8], [9], DSM is stable and fast because it does not require any additional operation such as generating a projection operator (MUSIC) or singular-value decomposition (LSM).

The authors have recently analyzed the structure of DSM and have proposed an improved version (DSMA) [9] for the 2D scalar inverse scattering problem. Beside this improvement we have also verified the correlation between DSM with Kirchhoff migration, which is one of the most popular techniques in geophysics area [10]. One of the goal of this work is to extend such an approach for the 3D inverse electromagnetic scattering problem for which we need to carefully handle the test function because of the vectorial aspect of the problem we are dealing with. In addition we believe that our extension is also connected with Kirchhoff migration type techniques such as reverse-time migration [11]. Numerical simulations are presented to verify our suggestion using synthetic data.

II. Forward Electromagnetic Scattering Problem

Here, we briefly introduce the forward electromagnetic scattering problem from small dielectric targets denoted as $\tau_m = \mathbf{r}_m + \alpha_m \mathbf{D}_m, \quad$ where $m = 1, 2, \cdots, M$, where $\mathbf{r}_m$ is the center, α_m is size, and $\mathbf{D}_m$ is the unit shape of each τ_m. We assume that each of τ_m is well-separated. We also denote the collection of τ_m as τ, i.e., $\tau = \bigcup_m \tau_m$. Through out this work, we focus on the permittivity contrast case, i.e., $\mu_0 = \mu_m$ where μ_0 and μ_m is magnetic permeability of background and τ_m, respectively.

The total electromagnetic fields $(\mathbf{E}(\mathbf{x}, \mathbf{y}), \mathbf{H}(\mathbf{x}, \mathbf{y}))$ are the solution of time-harmonic Maxwell's equation: The total electrical field can be expressed sum of incident field and scattered field, i.e., $\mathbf{E} = \mathbf{E}^i + \mathbf{E}^s$. In this paper, we consider the dipole transmitter. For uniqueness of solution, the scattered field satisfies following Silver-Möller radiation condition and can be represented as

$$\mathbf{E}^s(\mathbf{x}, \mathbf{y}) = \int_\Omega \underline{\mathbf{G}}(\mathbf{x}, \mathbf{r}) \mathbf{J}(\mathbf{r}, \mathbf{y}) \mathrm{d}\mathbf{r}, \tag{1}$$

where $\mathbf{J}_0(\mathbf{y})$ is current density. Here, $\underline{\mathbf{G}}(\mathbf{x}, \mathbf{z})$ is dyadic green function of time-harmonic Maxwell's equation which has the form of: $\underline{\mathbf{G}}(\mathbf{x}, \mathbf{y}) := \left(\underline{\mathbf{I}}_3 + \frac{1}{k_0} \nabla\nabla \right) g(\mathbf{x}, \mathbf{y})$ where $\underline{\mathbf{I}}_3$ is 3×3 unit matrix and $g(\mathbf{x}, \mathbf{y})$ is green function of 3D Helmholtz equation.

III. Direct Sampling method and its improvement

The DSM is recently developed non-iterative sampling type method for solving inverse scattering problem. For fixed dipole transmitter $\mathbf{y} \in \Gamma_t$, the scattered field data are measured at $\mathbf{x}_n$, $n = 1, 2, \cdots, N$ over the measurement simply connected surface (or curve) Γ_r and Ω_Γ is a domain enclosed by both Γ_r and Γ_t. Then, for sampling point $\mathbf{z} \in \Omega_\Gamma$, the indicator function of DSM for a fixed dipole transmitter is defined as

$$\mathcal{I}_{\mathrm{DSM}}(\mathbf{z}; \mathbf{y}) := \frac{\left| \langle \mathbf{E}^s(\mathbf{x}_n, \mathbf{y}), \underline{\mathbf{G}}(\mathbf{x}_n, \mathbf{z}) \mathbf{p}^{rt} \rangle_{L^2(\Gamma_r)} \right|}{\| \mathbf{E}^s(\mathbf{x}_n, \mathbf{y}) \|_{L^2(\Gamma_r)} \| \underline{\mathbf{G}}(\mathbf{x}_n, \mathbf{z}) \mathbf{p}^{rt} \|_{L^2(\Gamma_r)}}, \tag{2}$$

$$\mathcal{I}_{\text{DSMA}}(\mathbf{z}) := \frac{|\mathcal{L}(\mathbf{z})|}{\max|\mathcal{L}(\mathbf{z})|} \quad \text{where } \mathcal{L}(\mathbf{z}) = \left\langle \left\langle \mathbf{E}^s(\mathbf{x},\mathbf{y}), \underline{\mathbf{G}}(\mathbf{x},\mathbf{z})\mathbf{p}^{rt} \right\rangle_{L^2(\Gamma_r)}, \underline{\mathbf{G}}(\mathbf{y},\mathbf{z})\mathbf{p}^{tt} \cdot \mathbf{a} \right\rangle_{L^2(\Gamma_t)}. \tag{8}$$

where

$$\begin{aligned} \langle \mathbf{f}(\mathbf{x},\mathbf{y}), \mathbf{g}(\mathbf{x},\mathbf{y}) \rangle_{L^2(\Gamma_r)} &:= \int_{\Gamma_r} \mathbf{f}(\mathbf{x},\mathbf{y})\overline{\mathbf{g}(\mathbf{x},\mathbf{y})}\mathrm{d}S(\mathbf{x}) \\ \text{and } \|\mathbf{f}(\mathbf{x},\mathbf{y})\|_{L^2(\Gamma_r)} &:= \langle \mathbf{f}(\mathbf{x},\mathbf{y}), \mathbf{f}(\mathbf{x},\mathbf{y}) \rangle_{L^2(\Gamma_r)}. \end{aligned} \tag{3}$$

Here, $\mathbf{p}^{rt} \in \mathbb{S}^2$ is polarization of test dipole receiver, where $\mathbb{S}^2$ is unit sphere in $\mathbb{R}^3$. For the multiple dipole transmitters $\mathbf{y}_l \in \Gamma_t$, $l = 1, 2, \cdots, L$, the indicator function defined as $\mathcal{I}_{\text{DSM}}(\mathbf{z}) := \frac{1}{L}\sum_{l=1}^{L} \mathcal{I}_{\text{DSM}}(\mathbf{z}; \mathbf{y}_l)$. The main ideas of DSM is integral representation (1) and approximation formula: For extinct points $\mathbf{z}_1 \neq \mathbf{z}_2$ and closed simply curve Γ

$$\int_{\Gamma} \left(\underline{\mathbf{G}}(\mathbf{x},\mathbf{z}_1)\mathbf{p}, \overline{\underline{\mathbf{G}}(\mathbf{x},\mathbf{z}_2)}\mathbf{q} \right) \mathrm{d}S(\mathbf{x}) \approx \frac{1}{k_0} \left(\mathbf{p}, \mathrm{Im}\left(\underline{\mathbf{G}}(\mathbf{z}_1,\mathbf{z}_2)\mathbf{q} \right) \right) \tag{4}$$

where $\mathbf{p} \in \mathbb{C}^3$, $\mathbf{q} \in \mathbb{R}^3$. This means that

$$\begin{aligned} &\left\langle \mathbf{E}^s(\mathbf{x},\mathbf{y}), \underline{\mathbf{G}}(\mathbf{x},\mathbf{z})\mathbf{p}^{rt} \right\rangle_{L^2(\Gamma)} \\ &\approx \frac{1}{k_0} \sum_j |\tau_m| \left(\mathbf{J}(\mathbf{r}_m,\mathbf{y}), \mathrm{Im}\left(\underline{\mathbf{G}}(\mathbf{z},\mathbf{r}_m) \right) \mathbf{p}^{rt} \right). \end{aligned} \tag{5}$$

Due to a singular property of dyadic green function, the indicator function is reasonable.

To improve imaging performance, we suggest another indicator function for $\mathbf{p}^{tt} \in \mathbb{S}^2$ and $\mathbf{a} \in \mathbb{R}^3$ given by (8).

IV. Numerical Simulation

The scattered data is computed using *FEKO* at fixed frequency 749.481 MHz ($\lambda = 0.4\,\mathrm{m}$). The receivers are located on the surface of centered sphere with radius 2.5λ, $\theta_j = 5° + 10°(j-1)$, $j = 1, 2, \cdots, 18$ and $\phi_k = 10°(k-1)$, $k = 1, 2, \cdots, 36$ and measure electrical scattered data with respect to each directions ($\mathbf{x}_1, \mathbf{x}_2, \mathbf{x}_3$-directions). The dipole transmitters also located at the same angles than the receivers but with radius 2.475λ and are parallel to $\mathbf{x}_3$-axis. We consider single small dielectric sphere located at $\mathbf{r} = (0.25\lambda, 0.75\lambda, 0.5\lambda)$. The radius is $\alpha = 0.1\lambda$ and electric permittivity is $\varepsilon = 5\varepsilon_0$ within unbounded homogeneous space. The region of interest (ROI) Ω_Γ is defined as a cube of 2.5λ-side. DSM and DSMA have been applied using $\mathbf{p}^{rt} = \mathbf{p}^{tt} = [1, 1, 1]^T/\sqrt{3}$ and $\mathbf{a} = [1, 1, 1]^T$.

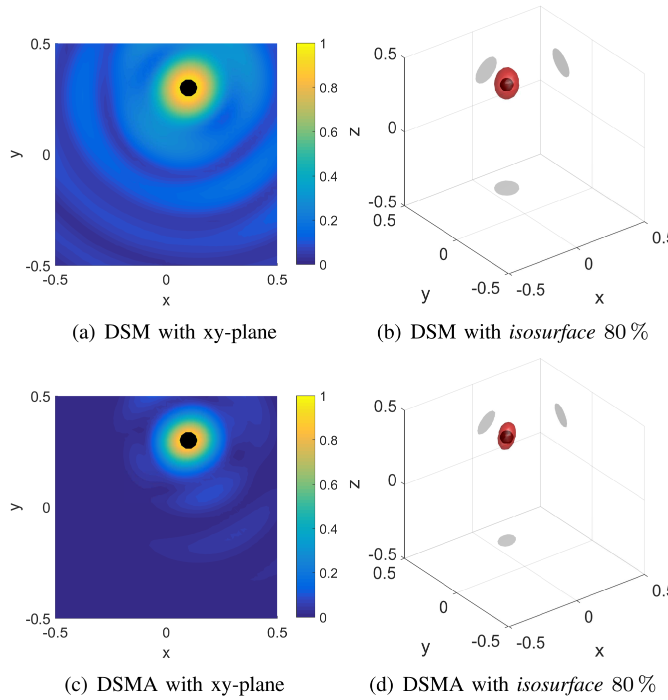

(a) DSM with xy-plane (b) DSM with *isosurface* 80 %

(c) DSMA with xy-plane (d) DSMA with *isosurface* 80 %

Fig. 1. Numerical results of DSM (top) and IDSM (bottom)

Figure 1 shows that the artifacts in the map of IDSM are much lower than the ones in the map of DSM leading to a better imaging performance.

V. Conclusion

In this work, an improvement of DSM for 3D inverse electromagnetic scattering problem is proposed. It shows an enhancement of the quality of the reconstruction via a decrease of the artifacts. The efficiency of the method is illustrated via numerical simulations.

In the forthcoming work a mathematical analysis of the indicator function will be considered and a comparison with the one obtained via the Kirchhoff migration will be proposed.

References

[1] S. Verma, S. Bhadauria, and S. Akhtar, "Review of nondestructive testing methods for condition monitoring of concrete structures," *J. Const. Eng*, 2013.

[2] M. Haynes, J. Stang, and M. Moghaddam, "Microwave breast imaging system prototype with integrated numerical characterization," *J. Biomed. Imag.*, vol. 2012, pp. 1–18, 2012.

[3] H. Ammari, E. Iakovleva, and D. Lesselier, "A MUSIC algorithm for locating small inclusions buried in a half-space from the scattering amplitude at a fixed frequency," *Multiscale Model. Sim.*, vol. 3, no. 3, pp. 597–628, 2006.

[4] R. Kress, "Inverse elastic scattering from a crack," *Inverse Prob.*, vol. 12, pp. 667–684, 1996.

[5] W.-K. Park, "Multi-frequency subspace migration for imaging of perfectly conducting, arc-like cracks in full- and limited-view inverse scattering problems," *J. Comput. Phys.*, vol. 283, pp. 52–80, 2015.

[6] K. Ito, B. Jin, and J. Zou, "A direct sampling method to an inverse medium scattering problem," *Inverse Prob.*, vol. 28, no. 2, p. 025003, 2012.

[7] ——, "A direct sampling method for inverse electromagnetic medium scattering," *Inverse Prob.*, vol. 29, no. 9, p. 095018, 2013.

[8] S. Kang, M. Lambert, and W.-K. Park, "Multi-frequency direct sampling method in inverse scattering problem," *J. Phys: Conf. Ser.*, vol. 904, no. 1, p. 012018, 2017.

[9] S. Kang, M. Lambert, and W.-K. Park, "Direct sampling method for imaging small dielectric inhomogeneities: analysis and improvement," *ArXiv e-prints*, p. 1801.05993, Jan. 2018.

[10] N. Bleistein, J. K. Cohen, W. John Jr *et al.*, *Mathematics of multidimensional seismic imaging, migration, and inversion*. Springer Science & Business Media, 2013, vol. 13.

[11] J. Chen, Z. Chen, and G. Huang, "Reverse time migration for extended obstacles: electromagnetic waves," *Inverse Problems*, vol. 29, no. 8, p. 085006, 2013.